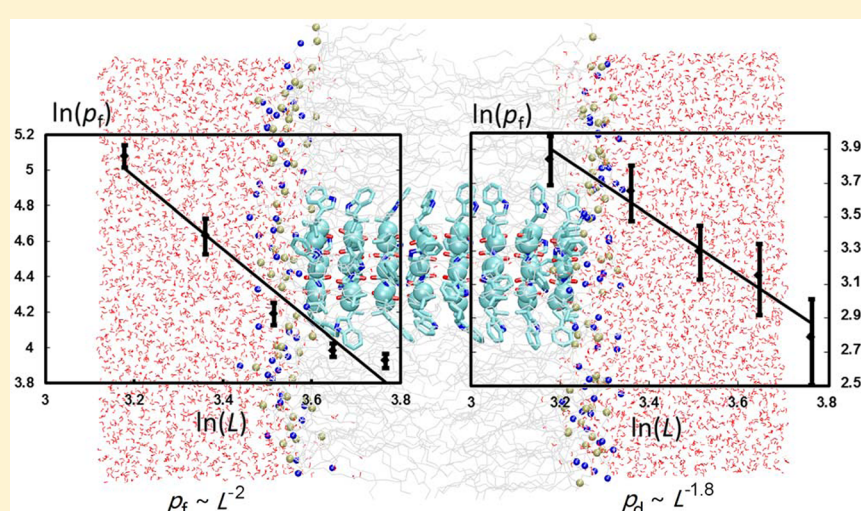


# Dependences of Water Permeation through Cyclic Octa-peptide Nanotubes on Channel Length and Membrane Thickness

Jian Liu,<sup>†,§</sup> Jianfen Fan,<sup>\*,†</sup> Min Cen,<sup>†</sup> Xuezeng Song,<sup>†</sup> Dongyan Liu,<sup>†</sup> Weiqun Zhou,<sup>†</sup> Zhao Liu,<sup>‡</sup> and Jianfeng Yan<sup>‡</sup>

<sup>†</sup>College of Chemistry, Chemical Engineering and Materials Science, <sup>‡</sup>College of Computer Science & Technology, Soochow University, Suzhou 215123, People's Republic of China

<sup>§</sup>Shanghai Institute of Applied Physics, Chinese Academy of Sciences, Shanghai 201800, People's Republic of China



**ABSTRACT:** Effects of the channel length and membrane thickness on the water permeation through the transmembrane cyclic octa-peptide nanotubes (octa-PNTs) have been studied by molecular dynamics (MD) simulations. The water osmotic permeability ( $p_f$ ) through the PNTs of  $k \times (WL)_4/\text{POPE}$  (1-palmitoyl-2-oleoyl-glycerophosphoethanolamine;  $k = 6, 7, 8, 9$ , and  $10$ ) was found to decay with the channel length ( $L$ ) along the axis ( $\sim L^{-2.0}$ ). Energetic analysis showed that a series of water binding sites exist in these transmembrane PNTs, with the barriers of  $\sim 3k_B T$ , which elucidates the tendency of  $p_f$  well. Water diffusion permeability ( $p_d$ ) exhibits a relationship of  $\sim L^{-1.8}$ , which results from the novel 1–2–1–2 structure of water chain in such confined nanolumens. In the range of simulation accuracy, the ratio ( $p_f/p_d$ ) of the water osmotic and diffusion permeability is approximately a constant. MD simulations of water permeation through the transmembrane PNTs of  $8 \times (WL)_4/\text{octane}$  with the different octane membrane thickness revealed that the water osmotic and diffusion permeability ( $p_f$  and  $p_d$ ) are both independent of the octane membrane thickness, confirmed by the weak and nearly same interactions between the channel water and octane membranes with the different thickness. The results may be helpful for revealing the permeation mechanisms of biological water channels and designing artificial nanochannels.

## INTRODUCTION

Transmembrane water channels play fundamental roles in organisms as well as in industrial applications.<sup>1,2</sup> The dynamics of water across nanochannels has significant implications for both the understanding of biological activities and designing of novel nanofluidic machines. Water molecules confined in nanochannels usually exhibit concerted permeation behaviors and density distribution patterns.<sup>3–9</sup> Intrinsic factors affecting water permeability include the geometry and structural stability of the channel, the channel–membrane match, and the channel–water interaction, etc. The present study focused on the effects of channel length and membrane thickness on the water osmotic permeability ( $p_f$ ) and diffusion permeability ( $p_d$ ),

both being means of quantifying water mobility inside a nanochannel.<sup>3,10–12</sup>

The osmotic permeability ( $p_f$ ) relates the net water flux through a channel due to the difference of the osmolyte concentrations (or the pressure difference) between the two reservoirs connected by the channel.<sup>3,13</sup> It is an intrinsic property of water mobility in a channel. Molecular dynamics (MD) simulations of water permeation in single-file ones through carbon nanotubes (CNTs)<sup>14</sup> and gramicidin-like helix peptide nanotubes<sup>15,16</sup> reveal no dependences of  $p_f$  on the

Received: April 15, 2012

Published: July 26, 2012



channel length. However, an exponential increase with the shortening of the channel was given for gramicidin derivatives by scanning electrochemical microscopy.<sup>17</sup> Nevertheless, Fang's group<sup>8</sup> reported that the single-file water flow in CNTs is found to decay with the channel length ( $\sim L^{-2.3}$ ), much faster than that ( $\sim L^{-1}$ ) predicted by a previous continuous-time random walk (CTRW) model<sup>4</sup> or assumed from the classic theory.<sup>18</sup>

The diffusion permeability ( $p_d$ ) represents the net water transport between the two reservoirs linked by a channel.<sup>3,15</sup> The dependences of  $p_d$  on channel length derived from the theoretical analyses and MD simulations are somewhat different. The theoretical prediction of the length-dependence of  $p_d$  is  $L^{-1}$  in macroscopic or multiple-file flow and  $L^{-2}$  in single-file flow.<sup>3</sup> However, Portella et al. reported that the single-file water diffusion permeability in gramicidin-like helix peptide nanotubes displays an inverse relationship with the length of the pore.<sup>15</sup>

Finally, the membrane thickness also affects the water permeation in a nanotube to some extent. Gong et al.<sup>19</sup> found that the outside structure greatly affects the water transport across the nanochannel. As the thickness of vacuum space membrane decreases, the flow and flux decrease.

It was reported that cyclic octa-peptides possess the optimum balance between the low-strain ring structures and the desired flat ring-shaped conformations.<sup>20</sup> The internal diameters of these cyclic octa-peptide nanotubes (octa-PNTs) are about 8 Å,<sup>20,21</sup> much closer to those of the widely studied SWCNT-(6,6) (single-wall carbon nanotube)<sup>8,19</sup> and Gramicidin A (GA).<sup>22</sup> However, two distinguished zones, i.e.,  $\alpha$ -plane and mid-plane zones, exist in the cyclic octa-PNTs.<sup>23</sup> The unique steric constraints of such nanochannels result in the distinguished wavelike pattern of a water chain, arraying in the form of 1–2–1–2 file, in contrast to single-file patterns in other nanochannels studied widely. How do the channel length and membrane thickness influence the water permeation in such nanochannels?

In this work, we designed a series of regularized cyclic octapeptides in a  $\beta$ -sheet folding<sup>20,21,23–26</sup> with an increasing number of rings and an octane slab with the different thickness to isolate the effects of channel length and membrane thickness on the water permeation inside octa-PNTs. Water energy profiles along the water pathway were evaluated to elucidate the molecular permeation mechanism. The influences of channel length and membrane thickness have been addressed to understand the main determinants of water permeation through octa-PNTs.

## THEORY, METHOD, AND MODELING DETAILS

**Permeability Coefficients.** The mobility of water molecules inside a channel can be quantified by the osmotic permeability ( $p_f$ ) and diffusion permeability ( $p_d$ ).<sup>3</sup> In particular,  $p_d$  is easily measured in an equilibrium MD simulation as<sup>11</sup>

$$p_d = q_0 v_w \quad (1)$$

where  $q_0$  is the rate of the unidirectional complete traversing of water in a channel, and  $v_w$  is the volume of a water molecule, with the constant of 30.5 Å<sup>3</sup>.

The  $p_f$  of a non-single-file channel can also be determined from an equilibrium MD simulation by the collective coordinate analysis.<sup>12</sup> The collective coordinate ( $n$ ) is defined as the time-dependent cumulative displacements of water molecules in a channel [S(t)], normalized to the channel length, as

$$dn = \sum_{i \in S(t)} dz_i / L \quad (2)$$

where  $L$  is the time-averaged channel length. In our practice, the integral-differential equation is taken in the following form<sup>26</sup>

$$\Delta_{t \rightarrow t+\Delta t} n = \sum_{\substack{i \in S(t) \\ i \in S(t+\Delta t)}} \Delta z_i / L + \frac{1}{2} \left( \sum_{\substack{i \in S(t) \\ i \notin S(t+\Delta t)}} + \sum_{\substack{i \notin S(t) \\ i \in S(t+\Delta t)}} \right) \Delta z_i / L \quad (3)$$

where  $\Delta t$  is the time interval between each frame of a MD trajectory. Here, 1.5 ps of  $\Delta t$  was used.

The collective coordinate ( $n$ ) was obtained by accumulating in every time step. The term  $n(t)$  describes the time-evolution of the permeation. At equilibrium,  $n(t)$  can be described as a one-dimensional unbiased random walk. The mean squared displacement (MSD) of  $n$ ,  $\langle n^2(t) \rangle$ , obeys the Einstein relation

$$\langle n^2(t) \rangle = 2D_n t \quad (4)$$

where  $D_n$  is the diffusion coefficient of  $n$ . The osmotic permeability ( $p_f$ ) can be calculated from

$$p_f = D_n v_w \quad (5)$$

**Modeling Systems and Details.** PNTs are a class of novel nanomaterials whose diameters and lengths can be controlled simply by adjusting the number of the employed amino acid residues. Composed of the amino acid residues Trp (W) and Leu (L), the PNTs possess the desired hydrophobic surface characteristics for embedding themselves into a lipid bilayer.<sup>25</sup> To understand the effect of channel length on the distinguished characteristics of the water permeability, five cyclic PNTs, i.e.,  $k \times (\underline{WL})_4$ ,  $k = 6, 7, 8, 9$ , and 10, were designed in this work, wherein the underlined letters correspond to the  $D$ -amino acids. The internal diameters of these nanotubes are about 8 Å and lengths span from 24 to 44 Å. POPE (1-palmitoyl-2-oleyl-glycerophosphoethanolamine) was selected to model the lipid bilayer of a membrane. The structure of  $8 \times (\underline{WL})_4$ /POPE was taken from our recent simulation result.<sup>23</sup> Those of 6, 7, 9, and  $10 \times (\underline{WL})_4$ /POPE were generated by replacing the  $8 \times (\underline{WL})_4$  PNT with the corresponding ones, respectively. Harmonic potentials with the force constant of 10 kcal mol<sup>-1</sup> Å<sup>-2</sup> were applied to the  $C_\alpha$  atoms of the PNT backbones to eliminate the tilt of the channels<sup>25,35</sup> and 1 kcal mol<sup>-1</sup> Å<sup>-2</sup> to the N and P atoms of the lipid to prevent the translation of the system. The four resultant systems were equilibrated by 10 ns with a time step of 1.0 fs using the NpT ensembles. The ratio of  $x$  and  $y$  dimensions was held constant, while the  $z$  dimension was allowed to vary under the imposed pressure. The  $z$ -dimensions of the periodic unitcells for these systems converged to 94–95 Å through the 30-ns equilibrium producing MD runs, which are long enough to compute water permeability from equilibrium simulations.<sup>11</sup>

For a controlled environment, it is necessary to adjust the membrane thickness according to the pore it accommodates. In this work, we devised an artificial membrane consisting of octane molecules,<sup>13</sup> which offers the possibility to modulate its thickness via molecular dynamics pressure coupling. First, a slab of 216, 252, or 288 octane molecules to prepare three membranes in a water box was equilibrated under constant temperature (310 K) and pressure (1 bar). The dimensions of  $x$  and  $y$  were fixed at 50 Å while the  $z$ -dimension was allowed to change freely to adjust the pressure. Then, a cylindrical vacuum

bubble with the radius of 10 Å was made to embed a  $8 \times (\text{WL})_4$  PNT. A 10-ns MD equilibration was performed using NpT ensemble. The resulted membrane thicknesses of the octane slabs with 216, 252, and 288 octane molecules are 31.0, 35.5, and 39.4 Å, respectively. The z-dimensions of the periodic unitcells for these systems converged to 85–86 Å through the 30-ns equilibrium producing MD runs.

The CHARMM27 force field<sup>27</sup> and TIP3P water model<sup>28</sup> were employed for all the MD simulations. The full electrostatic interactions were treated by the Particle Mesh Ewald (PME) approach.<sup>29</sup> Periodic boundary conditions were applied in three dimensions. The Nosé-Hoover Langevin piston method<sup>30</sup> was used to maintain the pressure of an MD simulation box at 1 bar, and Langevin dynamics was used to control the temperature at 310 K. All the simulations were performed with the program NAMD 2.7.<sup>31</sup> Analysis and visualization were made using the molecular graphics program VMD 1.8.7.<sup>32</sup> The rate of the unidirectional complete traversing of water in a channel,  $q_0$ , was determined by counting the average number of water molecules entering and leaving the channel in the whole trajectory. The slope of  $\text{MSD}_n$  vs t was taken from the linear interval, and  $D_n$  is 0.5 times of the resultant slope. The osmotic permeability ( $p_f$ ) and diffusion permeability ( $p_d$ ) were then computed by eqs 1 and 5.

## RESULTS AND DISCUSSION

**Dependence of Water Osmotic Permeability ( $p_f$ ) on Channel Length ( $L$ ).** Five structurally similar transmembrane PNTs,  $k \times \text{cyclo-(WL)}_4/\text{POPE}$  ( $k = 6, 7, 8, 9$ , and 10) were equilibrated and the resulted channel lengths are listed in Table 1, ranging from 24 to 44 Å. Water permeation through these five transmembrane PNTs have been simulated. As an example, the  $8 \times \text{cyclo-(WL)}_4/\text{POPE}$  system is illustrated in Figure 1a.

**Table 1. Unidirectional Complete Permeation Events ( $N_+$ ,  $N_-$ ), Rates ( $q_0$ ), Diffusion Permeability ( $p_d$ ), and Osmotic Permeability ( $p_f$ ) of Water Transportation in the Five Systems of  $k \times (\text{WL})_4/\text{POPE}$  ( $k = 6, 7, 8, 9$ , and 10) with the Different Channel Length ( $L$ )**

$k$	$L$ (Å)	$N_+$	$N_-$	$q_0$ (ns <sup>-1</sup> )	$p_d$ (Å <sup>3</sup> ns <sup>-1</sup> )	$p_f$ (Å <sup>3</sup> ns <sup>-1</sup> )
6	24.0	37	54	$1.53 \pm 0.23$	$46.7 \pm 6.9$	$160.6 \pm 10.2$
7	28.8	44	33	$1.27 \pm 0.21$	$38.6 \pm 6.3$	$102.7 \pm 10.1$
8 <sup>a</sup>	33.6	34	47	$0.89 \pm 0.14$	$27.1 \pm 4.3$	$66.1 \pm 4.1$
9	38.4	28	22	$0.83 \pm 0.17$	$23.4 \pm 4.9$	$53.9 \pm 2.1$
10	43.2	16	25	$0.53 \pm 0.13$	$16.3 \pm 4.1$	$50.8 \pm 2.0$

<sup>a</sup>Date of  $8 \times (\text{WL})_4$  were obtained from a 45-ns MD simulation, while the others were from 30-ns MD simulations

In an equilibrium MD running, the MSD curve of the collective coordination ( $\text{MSD}_n$ ) of the channel-water is linear with time. The  $\text{MSD}_n$  curves, given by the above five systems, are presented in Figure 2. The osmotic permeability ( $p_f$ ) was obtained from the slope of the  $\text{MSD}_n$  curve, based on the eqs 4 and 5. The results are listed in Table 1. The relationship of  $p_f \sim L$  is illustrated in Figure 3. Fitted with the logarithms of  $p_f$  and  $L$ , we found that within the studied range of channel length, the  $p_f$  value declines with the square of  $L$  ( $\sim L^{-2.0}$ ).

The present results are quite different from those reported. Darcy's Law describes the flow of a fluid through a porous medium to be inversely dependent on the length of two ends.<sup>33</sup> Textbook analysis carried out by Longuet-Higgins et al.<sup>34</sup> or Finkelstein<sup>3</sup> also gave a similar result. However, there are two

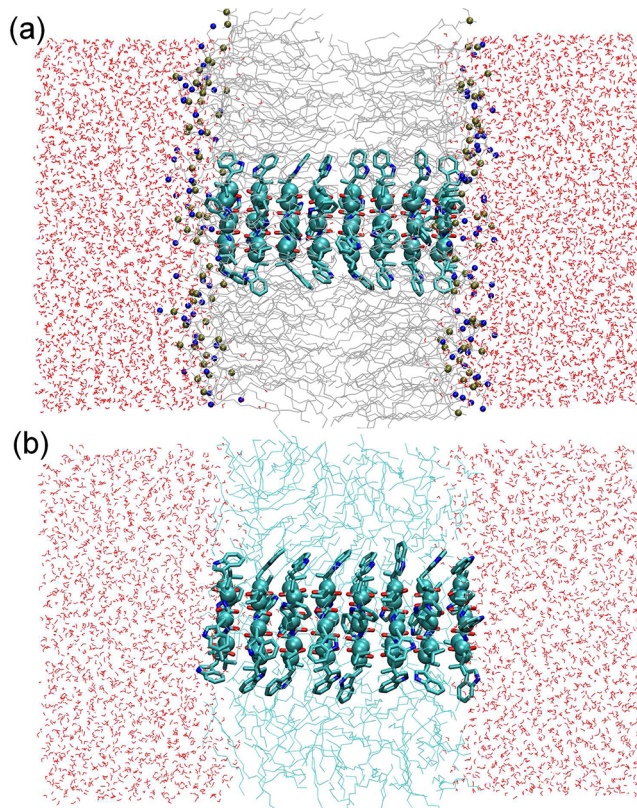


**Figure 1.** Snapshots of  $8 \times \text{cyclo-(WL)}_4$  PNT embedded in the fully hydrated POPE lipid bilayer (a) and octane slab (b). The C<sub>α</sub> atoms of the PNT backbone and N, P atoms of the lipid units are highlighted in vDW spheres, and hydrogen atoms are ignored for clarity.

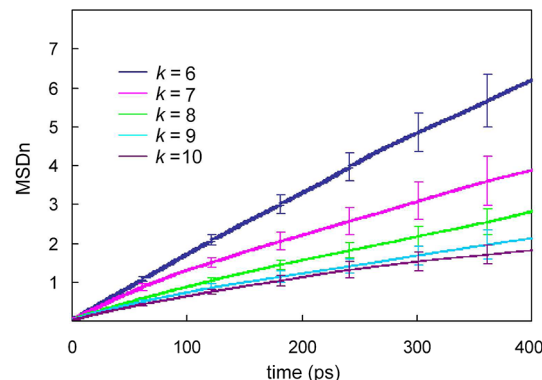


**Figure 2.**  $\text{MSD}_n$  curves of water permeation in the five transmembrane PNTs of  $k \times (\text{WL})_4/\text{POPE}$  ( $k = 6, 7, 8, 9$ , and 10) with different channel lengths. The slopes of the curves are directly proportional to the values of the osmotic permeability ( $p_f$ ) based on the Einstein relation  $\langle n^2(t) \rangle = 2D_n t$  and eq 5.

points worth noting in their analysis. One is the hypothesis that the friction force is uniform along the channel, and the other is the neglect of the interaction between water and channel. These two points of not enough detailed microperspectives lead the macroscopic results. In fact, when water molecules pass through a channel, they form strong interactions with the channel and transfer translational momentum to it. As the energy of motion dissipates to heat on the channel wall, friction rises. MD or Monte Carlo simulations<sup>8,14–16</sup> and experimental measurements<sup>17</sup> in recent years gave the different results, i.e., no dependences of  $p_f$  on the channel length,<sup>14–16</sup> an

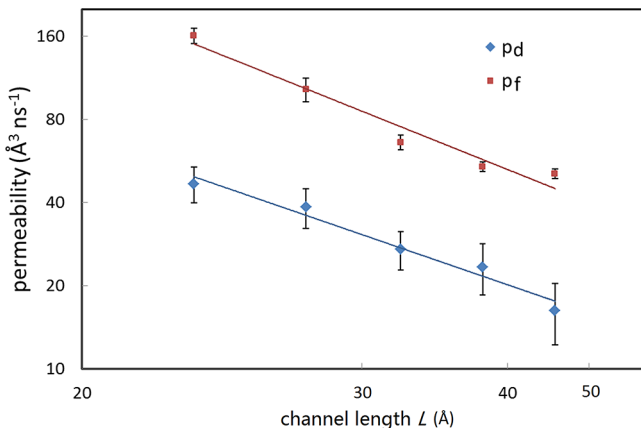


**Figure 3.** Bilogarithmic diagrams of the averaged osmotic permeability ( $p_f$ ) and diffusive permeability ( $p_d$ ) as the functions of the channel length ( $L$ ). The relationships between the simulated results of water permeation and channel length ( $L$ ) can be fitted to the functions with the powers of  $-2.0$  for  $p_f$  and  $-1.8$  for  $p_d$ , respectively.

exponential increase of  $p_f$  with the shortening of the channel,<sup>17</sup> or decay of  $p_f$  with the channel length ( $\sim L^{-2.3}$ ), etc. Nevertheless, most of these reported results are related to the single files of water chains, different from our distinguished 1–2–1–2 files.

To understand the mechanism underlying the numerical observations of the relationship between water mobility and channel length in our octa-PNTs, we have calculated the interaction potentials between a channel-water molecule and the peptide nanotube, membrane, and other water molecules, respectively, by averaging all the water molecules at each position along the channel. As shown in Figure 4, the curves

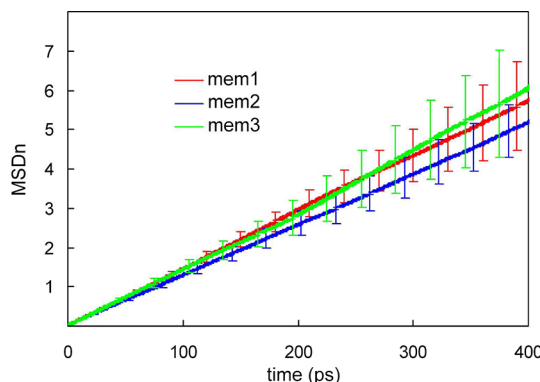


**Figure 4.**  $\text{MSD}_n$  curves in the three transmembrane PNTs of  $8 \times (\text{WL})_4/\text{octane}$  with the different membrane thickness of  $31.0$ ,  $35.5$ , and  $39.4 \text{ \AA}$ , denoted as mem1, mem2, and mem3, respectively. Error bars estimated from blocking methods are shown in vertical lines. The slopes of the curves are found nearly independent of the membrane thickness within the simulation accuracy.

describe that the fragments inside the inner part of the PNT channels fluctuate with a series of binding sites. Energy decomposition shows that water–water interaction (Figure 4d) is the main component of the total water energy profile, contributing  $5 \text{ kcal mol}^{-1}$  of barrier in channel. The water–channel component also affects the water energy profile in the channel, while the water–membrane interaction is very weak in the channel. The barriers in the individual mid-plane regions (zones between the two peptide rings) form the rate-limiting

determination for water permeation. The energy required for a water molecule to move from one binding site to the next within the PNT channel is  $\sim 3 k_B T$ . Increasing the number of cyclic peptide rings means adding new barriers. Such a result is quite different from those observed in helix-PNTs<sup>15</sup> and CNTs.<sup>14</sup> It was reported that, if the activation energy for a water–water displacement is higher than the thermal energy ( $k_B T$ ), including more barriers in the channel would lead to an exponential length dependence of  $p_f$ . As expected,  $p_f$  displays an inversely squared relationship with the length.

**Dependence of Water Diffusion Permeability ( $p_d$ ) on Channel Length ( $L$ ).** The diffusion permeability ( $p_d$ ) can be obtained by mirroring the complete permeation events<sup>3,11</sup> and computed from eq 1. The results are summarized in Table 1. The relationship of  $p_d \sim L$  is illustrated in Figure 3, giving the result of  $p_d \sim L^{-1.8}$ . In the range of MD simulation accuracy,  $p_d$  is approximately inversely squared with  $L$ .

Textbook analysis on the length-dependence of  $p_d$  gave  $L^{-1}$  in macroscopic or multiple-file flow and  $L^{-2}$  in single-file flow.<sup>3</sup> However, the recent MD and Monto Carlo simulations gave no dependence<sup>8</sup> or an inverse relationship of  $p_d$  on the channel length.<sup>15</sup>

The diffusion permeability ( $p_d$ ) represents the net water transportation in a channel. It is related with the water chain structure. The distribution profiles of water molecules along the nanotube axis of a cyclic octa-PNT propose a wavelike pattern of water–chain, arraying in the form of 1–2–1–2 file.<sup>23,24</sup> Such a novel 1–2–1–2 pattern was depicted in Figure 5, quite different from those of macroscopic flow as well as single-file flow. A strong correlation of water movement was also found in the 1–2–1–2 water chain, just like that in a single-file channel somehow. Figure 5 depicts the illustration of the “hopping” of a tracer water molecule through a cyclic octa-PNT in 1–2–1–2 file, with a vacancy in it. After each step that the tracer takes, it must wait until the vacancy has diffused the entire length of the channel, before it can advance to the another gap. Whereas in a macroscopic channel, even in a double-file one, the vacancy can diffuse in step with the tracer. Since the hopping rate from left to right is the same as that from right to left, in equilibrium, these two cases should have the same probabilities as a result of fineness equilibrium. Therefore, the vacancy position probabilities in all of the  $m$  gaps are the same. Thus, the rate of the tracer moves forward one gap in 1–2–1–2 file is proportional to  $1/m$  ( $m$  is the number of gaps), and therefore, its rate of advancing  $m$  steps is proportional to  $1/m^2$ . This is the molecular mechanism for the  $L^{-2}$  dependence of  $p_d$  in cyclic octa-PNTs, as in single-file channels.<sup>3</sup>

It is worth noting that the powers of  $-2.0$  and  $-1.8$  in Figure 3 have some uncertainty somehow. Therefore, they do not absolutely proclaim that the length dependence of  $p_d$  is weaker than that of  $p_f$ . On the other hand, our result is only valid for the studied range of channel length.

**Dependence of Water Permeation on Membrane Thickness.** Three structurally similar transmembrane PNTs,  $8 \times \text{cyclo-(WL)}_4/\text{octane}$  with the number of octane molecules of 216, 252, and 288 (denoted as mem1, mem2, and mem3), respectively, were equilibrated. The resulting membrane thicknesses are  $31.0$ ,  $35.5$ , and  $39.4 \text{ \AA}$ , respectively, listed in Table 2. Water permeation through these three transmembrane PNTs has been simulated. As an example, one of the three systems is illustrated in Figure 1b. The water osmotic permeability ( $p_f$ ) and diffusion permeability ( $p_d$ ) in these three systems with the different membrane thickness have been

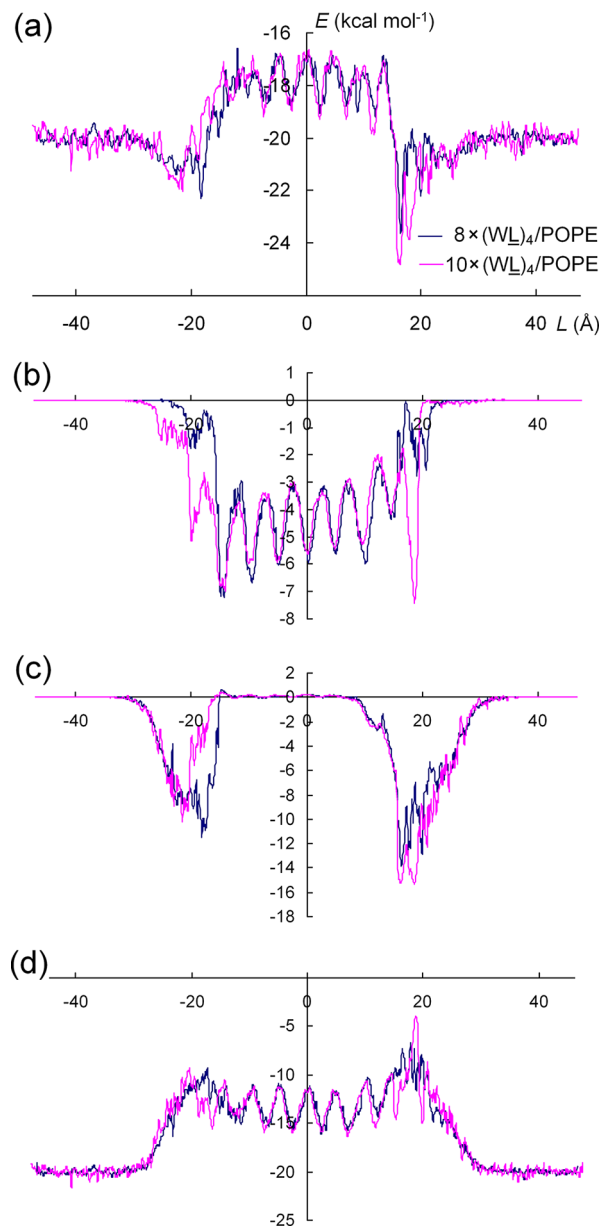


**Figure 5.** Energy profiles of a water molecule in  $8 \times (\text{WL})_4/\text{POPE}$  and  $10 \times (\text{WL})_4/\text{POPE}$  (a) and the interactions of water–channel (b), water–membrane (c), and water–water (d). The results in other titled PNTs are similar. Peaks of water–water profiles exist in the mid-plane regions where only two H-bonds could be formed by each channel water molecule while four in the  $\alpha$ -plane regions.<sup>21</sup>

**Table 2. Membrane Thickness, Diffusion and Osmotic Permeability ( $p_d$ ,  $p_f$ ) for the Three Transmembrane PNTs of  $8 \times (\text{WL})_4/\text{octane}$  with the Different Octane Membrane Thickness, Denoted as mem1, mem2, and mem3, Respectively**

systems	thickness (Å)	$p_d$ (Å <sup>3</sup> ns <sup>-1</sup> )	$p_f$ (Å <sup>3</sup> ns <sup>-1</sup> )
mem1	31.0	$43.7 \pm 6.7$	$223 \pm 12$
mem2	35.5	$44.7 \pm 6.7$	$200 \pm 11$
mem3	39.4	$46.7 \pm 6.9$	$221 \pm 15$
lipid <sup>a</sup>	~38	$27.1 \pm 4.3$	$66.0 \pm 4.0$

<sup>a</sup>Data of the lipid system are just the records of  $k = 8$  in Table 1. A tiny difference of  $p_f$  comes from the different selected linear interval of  $\text{MSD}_n$  vs  $t$ .

checked. Three  $\text{MSD}_n$  curves presented in Figure 6 show no distinct differences. From the slopes of  $\text{MSD}_n$  curves and

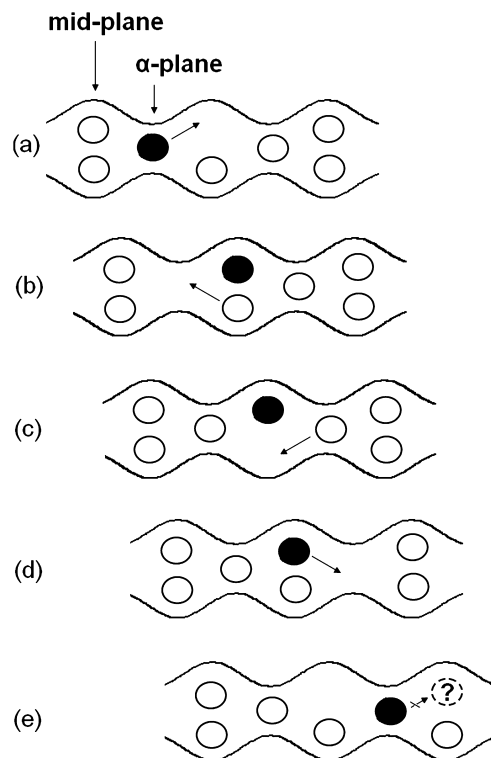


**Figure 6.** Illustration of the “hopping” of a tracer water molecule in 1–2–1–2 file, with a vacancy in it. Once the tracer has advanced to a mid-plane region, it must wait for the vacancy to move forward the entire length of the channel before it can advance to the next gap.

complete permeation events, we got the values of  $p_f$  and  $p_d$  in the three systems. The results are summarized in Table 2, showing no distinct dependence of  $p_f$  and  $p_d$  on the thickness of the octane membrane.

In practical applications, the structure outside a macroscopic or mesoscopic channel is usually insignificant.<sup>36</sup> However, those affects on the permeation of water across a nanochannel have rarely been reported. Gong et al.<sup>19</sup> reported that the thickness of the external vacuum space membrane of a CNT could affect water permeation somehow. The interaction between the water molecules inside and outside the channel influences the water transportation. In our system, decomposition of energy shows that the interaction between the channel-water and octane membrane is very weak and nearly insensitive to the membrane thickness (Figure 7). Therefore, the membrane thickness has little effect on the water permeability, which is consistent to Gong’s conclusion<sup>19</sup> for the case of the membrane thickness close to the channel length.

Nevertheless, the octane membrane is a little different from the phospholipid membrane, and the simulation studies of the phospholipid membrane have identified a strong influence on water–membrane interaction caused by the interactions of lipid headgroups with water molecules at the channel entrance (Figure 4c). The two permeability coefficients ( $p_f$  and  $p_d$ ) of  $8 \times \text{cyclo-(WL)}_4$  in the octane slab are much larger than those in phospholipid membrane (see Table 2). Therefore, it would be interesting to systematically explore the effects of the surrounding phospholipid membrane.

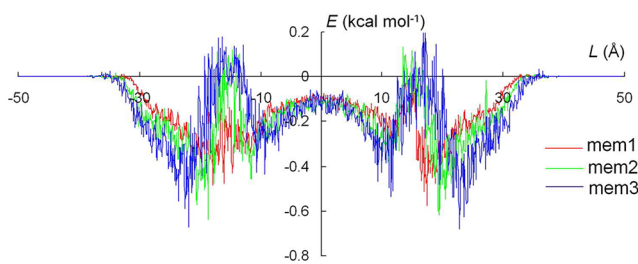


**Figure 7.** Energy profiles of water–octane interactions in the three transmembrane PNTs of  $8 \times (\text{WL})_4/\text{octane}$  with the different membrane thickness of 31.0, 35.5, and 39.4 Å, denoted as mem1, mem2, and mem3, respectively. These curves show no distinct differences and the energy barriers are much less than those of water–peptide and water–water interactions shown in Figure 4. The result indicates that the thickness of an octane membrane is not the key factor of water permeation.

## CONCLUSION

Taking advantage of computer modeling, a series of cyclic D,L-peptide channels of different length with directly comparable structural features embedded in membranes were designed and characterized using all atomic molecular dynamics simulations to address the water permeation determinations. The analysis of water mobility reveals that the diffusion permeability ( $p_d$ ) and osmotic permeability ( $p_f$ ) are both approximately inversely squared dependent on the channel length. This result varies from the textbook analysis<sup>3</sup> or early simulation results.<sup>8,14–16</sup> The dependence of  $p_f$  on the channel length comes from the momentum dissipation through the strong interactions between the channel wall and water molecules, and that of  $p_d$  results from the novel 1–2–1–2 water chain structure in the confined cyclic octa-PNTs. The permeation of 1–2–1–2 water chain in PNTs is much different from that of single-file ones as well as macroscopic flow. This implies that the structure of the water channel is the major determinant underlying water permeability. Nevertheless, the thickness of an octane membrane is insignificant for water permeation. However, the water permeation across a phospholipid membrane may be somewhat different from that across an octane membrane. The critical factor affecting water permeation is the type of membrane rather than its thickness.

Our finding may be helpful for providing insights of permeation mechanism of biological water channels and designing artificial nanochannels.

## AUTHOR INFORMATION

### Corresponding Author

\*Telephone: 0086-0512-65883271. E-mail: jffan@suda.edu.cn.

### Notes

The authors declare no competing financial interest.

## ACKNOWLEDGMENTS

This work has been supported by the National Natural Science Foundation of China (Grant No. 21173154) and the Priority Academic Program Development of Jiangsu Higher Education Institutions. The authors are grateful to Dr. Xiaojing Gong for her insightful discussions and indebted to School of Computer Science & Technology in Soochow University for providing us generous amounts of computer facilities assignment on their high-powered computers.

## REFERENCES

- (1) Agre, P. Aquaporin water channels (Nobel lecture). *Angew. Chem., Int. Ed.* **2004**, *43*, 4278–4290.
- (2) Shannon, M. A.; Bohn, P. W.; Elimelech, M.; Georgiadis, J. G.; Mariñas, B. J.; Mayes, A. M. Science and technology for water purification in the coming decades. *Nature* **2008**, *452*, 301–310.
- (3) Finkelstein, A. *Water movement through lipid bilayers, pores, and plasma membranes*; John Wiley & Sons, New York, 1987.
- (4) Hummer, G.; Rasaiah, J. C.; Noworyta, J. P. Water conduction through the hydrophobic channel of a carbon nanotube. *Nature* **2001**, *414*, 188–190.
- (5) Fang, H.; Wan, R.; Gong, X.; Lu, H.; Li, S. Dynamics of single-file water chains inside nanoscale channels: physics, biological significance and applications. *J. Phys. D: Appl. Phys.* **2008**, *41*, 103002.
- (6) Berezhkovskii, A.; Hummer, G. Single-file transport of water molecules through a carbon nanotube. *Phys. Rev. Lett.* **2002**, *89*, 064503.
- (7) Sokhan, V. P.; Nicholson, D.; Quirke, N. Fluid flow in nanopores: Accurate boundary conditions for carbon nanotubes. *J. Chem. Phys.* **2002**, *117*, 8531–8539.
- (8) Li, J.; Yang, Z.; Fang, H.; Zhou, R.; Tang, X. Effect of the carbon-nanotube length on water permeability. *Chin. Phys. Lett.* **2007**, *24*, 2710–2713.
- (9) Thomas, J. A.; McGaughey, A. J. H. Water flow in carbon nanotubes: transition to subcontinuum transport. *Phys. Rev. Lett.* **2009**, *102*, 184502.
- (10) Zhu, F.; Tajkhorshid, E.; Schulten, K. Pressure-induced water transport in membrane channels studied by molecular dynamics. *Biophys. J.* **2002**, *83*, 154–160.
- (11) Zhu, F.; Tajkhorshid, E.; Schulten, K. Theory and simulation of water permeation in Aquaporin-1. *Biophys. J.* **2004**, *86*, 50–57.
- (12) Zhu, F.; Tajkhorshid, E.; Schulten, K. Collective diffusion model for water permeation through microscopic channels. *Phys. Rev. Lett.* **2004**, *93*, 224501.
- (13) Zelenina, M.; Brismar, H. Osmotic water permeability measurements using confocal laser scanning microscopy. *Eur. Biophys. J.* **2000**, *29*, 165–171.
- (14) Kalra, A.; Garde, S.; Hummer, G. Osmotic water transport through carbon nanotube membranes. *Proc. Natl. Acad. Sci. U.S.A.* **2003**, *100*, 10175–10180.
- (15) Portella, G.; Pohl, P.; de Groot, B. L. Invariance of single-file water mobility in Gramicidin-like peptidic pores as function of pore length. *Biophys. J.* **2007**, *92*, 3930–3937.
- (16) Portella, G.; de Groot, B. L. Determinants of water permeability through nanoscopic hydrophilic channels. *Biophys. J.* **2009**, *96*, 925–938.
- (17) Saparov, S. M.; Pfeifer, J. R.; Al-Momani, L.; Portella, G.; de Groot, B. L.; Koert, U.; Pohl, P. Mobility of a one-dimensional confined file of water molecules as a function of file length. *Phys. Rev. Lett.* **2006**, *96*, 148101.
- (18) Finkelstein, A.; Rosenberg, P. Single-file transport: implications for ion and water movement through gramicidin A channels. *Membr. Transp. Processes* **1979**, *3*, 77–88.
- (19) Gong, X.; Li, J.; Zhang, H.; Wan, R.; Lu, H.; Wang, S.; Fang, H. Enhancement of water permeation across a nanochannel by the structure outside the channel. *Phys. Rev. Lett.* **2008**, *101*, 257801.
- (20) Okamoto, H.; Nakanishi, T.; Nagai, Y.; Kasahara, M.; Takeda, K. Variety of the molecular conformation in peptide nanorings and nanotubes. *J. Am. Chem. Soc.* **2003**, *125*, 2756–2769.
- (21) Ghadiri, M. R.; Granja, J. R.; Milligan, R. A.; McRee, D. E.; Khazanovich, N. Self-assembling organic nanotubes based on a cyclic peptide architecture. *Nature* **1993**, *366*, 324–327.
- (22) de Groot, B. L.; Tielemans, D. P.; Pohl, P.; Grubmüller, H. *Biophys. J.* **2002**, *82*, 2934.
- (23) Liu, J.; Fan, J.; Tang, M.; Zhou, W. Molecular Dynamics simulation for the structure of the water chain in a transmembrane peptide nanotube. *J. Phys. Chem. A* **2010**, *114*, 2376–2383.
- (24) Engels, M.; Bashford, D.; Ghadiri, M. R. Structure and dynamics of self-assembling peptide nanotubes and the channel-mediated water

- organization and self-diffusion. A molecular dynamics study. *J. Am. Chem. Soc.* **1995**, *117*, 9151–9158.
- (25) Tarek, M.; Maigret, B.; Chipot, C. Molecular dynamics investigation of an oriented cyclic peptide nanotube in DMPC bilayers. *Biophys. J.* **2003**, *85*, 2287–2298.
- (26) Liu, J.; Fan, J.; Tang, M.; Cen, M.; Yan, J.; Liu, Z.; Zhou, W. Water diffusion behavior and transportation properties in transmembrane cyclic hexa-, octa- and decapeptide nanotubes. *J. Phys. Chem. B* **2010**, *114*, 12183–12192.
- (27) MacKerell, A. D.; Bashford, D.; Bellott, M.; Dunbrack, R. L.; Evanseck, J. D.; Field, M. J.; Fischer, S.; Gao, J.; Guo, H.; Ha, S.; Joseph-McCarthy, D.; Kuchnir, L.; Kuczera, K.; Lau, F. T. K.; Mattos, C.; Michnick, S.; Ngo, T.; Nguyen, D. T.; Prodhom, B.; Reiher, W. E., III; Roux, B.; Schlenkrich, M.; Smith, J. C.; Stote, R.; Straub, J.; Watanabe, M.; Wiorkiewicz-Kuczera, J.; Yin, D.; Karplus, M. All-atom empirical potential for molecular modeling and dynamics Studies of proteins. *J. Phys. Chem. B* **1998**, *102*, 3586–3616.
- (28) Jorgensen, W. L.; Chandrasekhar, J.; Madura, J. D.; Impey, R. W.; Klein, M. L. Comparison of simple potential functions for simulating liquid water. *J. Chem. Phys.* **1983**, *79*, 926–935.
- (29) Darden, T. A.; York, D. M.; Pedersen, L. G. Particle mesh Ewald: an N-log(N) method for Ewald sums in large systems. *J. Chem. Phys.* **1993**, *98*, 10089–10092.
- (30) Martyna, G. J.; Tobias, D. J.; Klein, M. L. Constant pressure molecular dynamics algorithms. *J. Chem. Phys.* **1994**, *101*, 4177–4189.
- (31) Phillips, J. C.; Braun, R.; Wang, W.; Gumbart, J.; Tajkhorshid, E.; Villa, E.; Chipot, C.; Skeel, R. D.; Kalé, L.; Schulten, K. Scalable molecular dynamics with NAMD. *J. Comput. Chem.* **2005**, *26*, 1781–1802.
- (32) Humphrey, W.; Dalke, A.; Schulten, K. VMD: visual molecular dynamics. *J. Mol. Graphics* **1996**, *14*, 33–38.
- (33) Bear, J. *Dynamics of fluids in porous media*; American Elsevier: New York, 1992.
- (34) Longuet-Higgins, H. G.; Austin, G. The kinetics of osmotic transport through pores of molecular dimensions. *Biophys. J.* **1966**, *6*, 217–224.
- (35) Holt, A.; Killian, J. A. Orientation and dynamics of transmembrane peptides: the power of simple models. *Eur. Biophys. J.* **2010**, *39*, 609–621.
- (36) Whitby, M.; Quirke, N. Fluid flow in carbon nanotubes and nanopipes. *Nat. Nanotechnol.* **2007**, *2*, 87–94.